Expanding the toolbox of probiotic *Escherichia coli* Nissle 1917 for synthetic biology

Fang Ba, Yufei Zhang, Xiangyang Ji, Wan-Qiu Liu, Shengjie Ling, and Jian Li*

School of Physical Science and Technology, ShanghaiTech University, Shanghai, 201210, China

*Corresponding author. Email: lijian@shanghaitech.edu.cn (J.L.)

Abstract

Escherichia coli Nissle 1917 (EcN) is a probiotic microbe that has the potential to be developed as a promising chassis for synthetic biology applications. However, the molecular tools and techniques for utilizing EcN have not been fully explored. To address this opportunity, we systematically expanded the EcN-based toolbox, enabling EcN as a powerful platform for more applications. First, two EcN cryptic plasmids and other compatible plasmids were genetically engineered to enrich the manipulable plasmid toolbox for multiple gene coexpression. Next, we developed two EcN-based enabling technologies, including the conjugation strategy for DNA transfer, and quantification of protein expression capability. Finally, we expanded the EcN-based applications by developing EcN native integrase-mediated genetic engineering capabilities and establishing an *in vitro* cell-free protein synthesis (CFPS) system. Overall, this study expanded the toolbox for manipulating EcN as a commonly used probiotic chassis, providing several simplified, dependable, and predictable strategies for researchers working in synthetic biology fields.

Keywords: synthetic biology, probiotic engineering, *Escherichia coli* Nissle 1917, cryptic plasmid, integrase, cell-free protein synthesis

Introduction

Microbes are widely used for molecule biosynthesis and biomanufacturing purposes.[1,2] Specifically, genetically engineered microbes can be used for the "Design-Build-Test-Learn" cycle,[3,4] including laboratory research,[5,6] industrial production,[7] and biomedical living therapeutics.[8–10] As a result, probiotics are excellent microorganism candidates due to their high-biosecurity, non-toxicity, biocompatibility, and well-acceptability.[10,11] Several probiotics, including gram-positive bacteria (e.g., *Bifidobacterium bifidum*,[12] *Lactobacillus lactis*,[10,13] and *Streptococcus thermophilus*[14]) and gram-negative bacteria (e.g., *Bacteroides fragilis*[10]), have been isolated, engineered, and used as living factories. In addition, these chasses have been used in the biosensing,[5] biomolecule production and delivery,[15] metabolic regulation,[16] antitumor therapy,[17] and immunotherapy.[18]

Nonetheless, *Escherichia coli* Nissle 1917 (EcN) has been among the most widely used and acceptable strains since it was identified in 1917.[19] Due to its unique superiority, such as its well-understood *Escherichia coli* background, long-term biosecurity record of human administration, great *in vivo* colonization ability, antagonistic, anti-inflammatory, and anti-invasive activity,[20] EcN was utilized as both a laboratory chassis cell and a commercial probiotic product named "Mutaflor".[19] Up to now, EcN has become one of the most popular probiotic chassis for developing living therapeutics in pathogenic infections,[21] metabolic regulation,[16] GI tract inflammations,[15] and antitumor treatments.[22]

Nowadays, some EcN-based genetic engineering strategies, including genome engineering (e.g., Lambda-Red recombination,[23] integrase-based site-specific recombination,[24] and CRISPR-Cas-based gene editing technologies[25–27]), cryptic plasmid engineering,[25–27] and

chassis modification,[24,28] have been designed, built, and tested. However, the genetic engineering toolbox of EcN can be further expanded in other fields due to its non-type strain properties.

To further meet these demands, EcN-based genetic engineering toolbox was systematically enriched to expand probiotic-based synthetic capabilities. First, EcN cryptic plasmids and other synthetic plasmids were modified to enrich the vector toolbox. In details, the two EcN cryptic plasmids pMUT1 and pMUT2 were successfully minimized, and the minimized pMUT2 origin of replication (oriV) was characterized as a 26 bp DNA sequence. Next, the coexistence and curing of up to four compatible plasmids were demonstrated, including oriVs of ColE1, ColE2, p15A, pSC101, and incW. Second, two EcN-enabling technologies were developed for DNA and protein manipulation. A simplified plasmid transfer strategy was developed (at least 30 minutes) via bacterial conjugation, which providing another efficient way than chemical or electrical transformation. Besides, EcN protein expression capability was quantified using three generalized genetic circuits, sfGFP expression ranged from 0.24 to 44.7 μg / mL. Third, two EcN-inspired applications were developed for potential probiotic functionalization. On the one hand, four new integrases in the EcN genome were first characterized, and the integrases were expressed and used for deletion, inversion, and integration depending on the designed *attP* / *attB* orientations. On the other hand, probiotic EcN-based cell-free protein synthesis (CFPS) system was successfully established (sfGFP yield reached approximately 160.8 μg / mL). In addition, lyophilized EcN CFPS systems retained acceptable activity within seven days.

We expanded the EcN-based genetic engineering toolbox for desired applications. It is worth emphasizing that four probiotic-derived integrases were first characterized as reliable

genetic engineering tools for probiotic chassis modification. In addition, a probiotic-based CFPS system was successfully established for on-demand biomanufacturing of pharmaceutical proteins, vaccines, and drug production. Therefore, this study may inspire the engineering of more probiotics for broad applications in synthetic biology, metabolic engineering, and biomedical engineering.

Results and Discussion

Minimization of EcN Cryptic Plasmids pMUT1 and pMUT2

EcN contains two cryptic plasmids pMUT1 (3173 bp) and pMUT2 (5514 bp), which are not transmissible and without antibiotic resistance genes (**Figures S1A, B**).[25] Although these plasmids have been modified and functionalized as synthetic vectors for specific purposes,[25–27] they have not been comprehensively explored, such as their minimized size (**Figure 1A**). To address these issues, we initially analyzed plasmid sequences and annotations of putative open reading frames (ORFs) (**Figure S1B**). After deleting redundant sequences, pMUT1 was partially truncated from 3173 bp to 1312 bp (**Figure 1B**), while pMUT2 was truncated from 5514 bp to 3093 bp (**Figure 1C**). Next, the two truncated vectors were reconstructed with antibiotic resistance genes, and their existence stability was verified. Referring to previous reports, pMUT1 contains ColE1-like oriV, which is commonly derived as plasmid vectors (e.g., pET-series, pSB1C3, pJL1),[25] but pMUT2 is mostly homologous to plasmid pUB6060 from *Plesiomonas shigelloides* and annotated as a ColE2-like oriV, which has not been comprehensively explored before.[25,29] Hence, to further minimized pMUT2 and precisely identified its oriV sequence, we performed truncation experiments and ensured its oriV

sequence was 26 bp (**Figure S1C**). Lastly, to conveniently integrate gene of interests (GOI) into the truncated pMUT plasmids, we added BioBrick prefix and BioBrick suffix sequences into variants and finally constructed the minimized pMUT plasmids: pMUT1-mini (2423 bp) (**Figure 1B**) and pMUT2-mini (3136 bp) (**Figure 1C**).[30] Furthermore, the modified plasmids were analyzed via agarose gel electrophoresis and correctly sequenced (**Figure 1D**, and **Figure S1D**). In summary, we successfully minimized two EcN cryptic plasmids, precisely identified ColE2-like oriV sequence, and constructed two pMUT-based minimized plasmids.

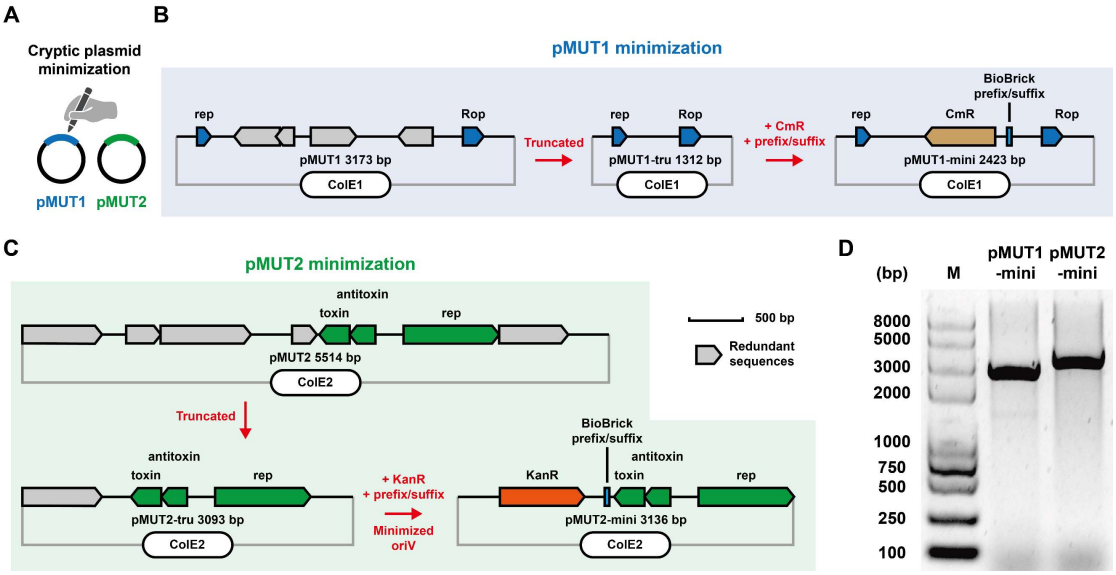

Figure 1. Minimization of cryptic plasmids.
(A) Wild type EcN contains two cryptic plasmids pMUT1 and pMUT2.
(B) Workflow of pMUT1 minimization. pMUT1-tru was truncated from pMUT1 by redundant sequence deletion, pMUT1-mini was derived from pMUT1-tru by adding antibiotic resistance gene CmR and BioBrick prefix / suffix sequences.
(C) Workflow of pMUT2 minimization. pMUT2-tru was truncated from pMUT2 by redundant sequence deletion, pMUT2-mini was derived from pMUT2-tru by adding antibiotic resistance gene KanR and BioBrick prefix / suffix sequences.
(D) Agarose gel electrophoresis of two minimized plasmids that linearized by FastDigest XbaI digestion.

Coexistence and Curing of Compatible Plasmids in EcN

The maximum number of coexistent pairs of engineered plasmids was explored after the characterization of the compatible cryptic plasmids, notably, the oriV is crucial for plasmid existence in microbes. oriV is classified as different incompatibility groups depending on the replication mechanism, indicating that two different plasmids with the same oriV cannot coexist in one microbe because of the competence of the same replication machine since they may create an unpredictable environment.[31] Therefore, establishing compatible plasmid vectors can expand the exogenous DNA capacity in one strain for synchronous gene expression. To meet these demands, a series of empty vectors (followed as iGEM BioBrick assembly standard[30]) mainly consisting of four parts (antibiotic resistance gene, oriV, BioBrick prefix / BioBrick suffix (for molecular cloning), and GOI) were developed (**Figure 2A**). The orthogonal and compatible plasmid groups in EcN were then assembled to follow the basic design that six plasmid vectors were constructed using four antibiotic resistance genes and five oriVs (**Figure 2B**, and **Figure S2**). When plasmids were successfully constructed in *E. coli* Mach1-T1, they were then transformed into wild type EcN and their copy number was quantified via qPCR. The results showed that pMUT2-mini (ColE2) had the highest copy number of ~22 per cell, while pFB2 (pSC101) had the lowest copy number (~2 per cell) (**Figure 2C**). Next, we gained four EcN strains that contain four compatible vectors, respectively. After seven days' continuous culture, the EcNs did not lose the vectors and could normally grow on LB-agar plates (with four antibiotics) (**Figure 2D**). In addition, these vectors could be cured using spCas9-based gene editing tools as previously reported,[32] which expanding the plasmid manipulation method in EcN. In conclusion, we expanded the compatible plasmid vectors for EcN and demonstrated

their coexistence capability for at least one week.

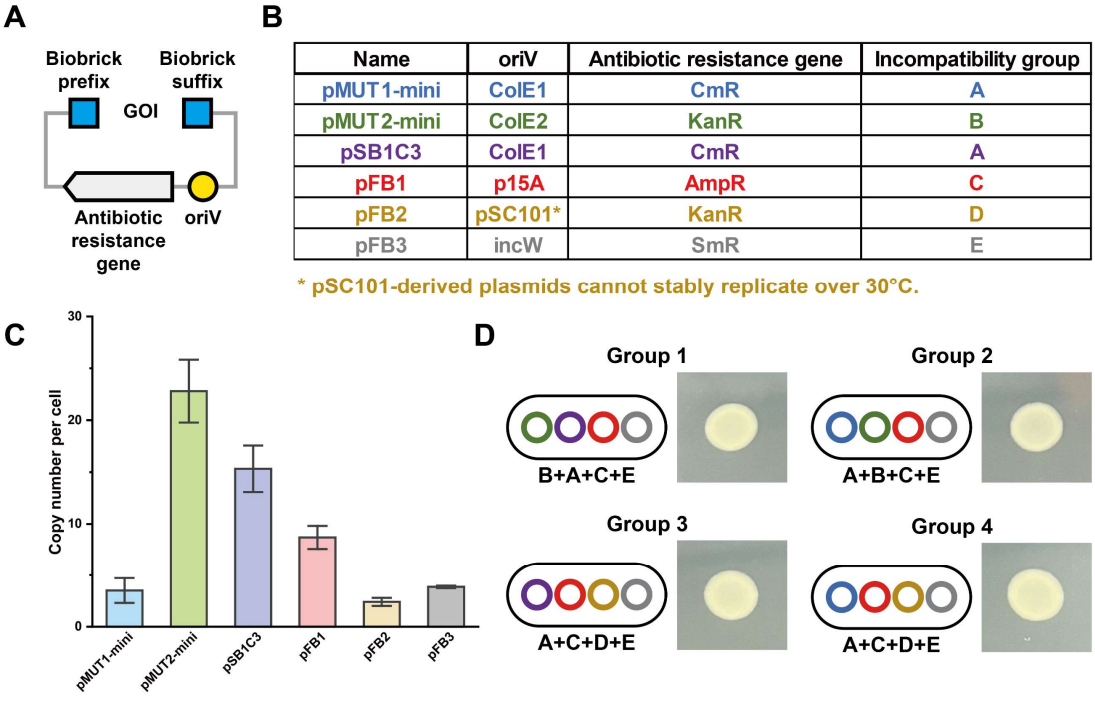

Figure 2. Coexistence of compatible plasmids in EcN.
(A) Schematic design of compatible plasmid vectors. GOI (gene of interests) can be inserted into vectors by molecular cloning via BioBrick prefix / suffix sites.
(B) Classification of vectors.
(C) Copy number per EcN cell of six vectors. Each value (mean ± standard deviation, SD) was calculated with three biological replicates.
(D) Compatible vectors were coexistent in EcN. All groups contained up to four compatible vectors in one strain, and could grow normally on LB-agar plates (with four antibiotics) after seven days' cultivation. The experiments were performed as thrice with the same results.

Bacterial Conjugation

So far, EcN-based chassis modification was performed by plasmid engineering. Next, we focused on the enabling technology to render EcN new properties and functionalities. It was worth noting that the EcN-based conjugation method for DNA transfer has not been commonly developed. Herein, a simplified strategy was developed for expanding EcN-based enabling technology.

Bacterial conjugation is one of the powerful tools of horizontal gene transfer within microbial communities, which enables donor strains to transfer their DNA through conjugative pili and the DNA was received by recipients.[33] This strategy has been developed for bacteria-bacteria DNA transfer within different species.[34] Depending on our previous attempts, the calcium chloride-based heat-shock transformation strategy was unsuccessful for EcN (data not shown). Besides, the efficiency of electroporation-based transformation is not high enough compared with the generally used laboratory *E. coli* strains, such as DH5α (**Figure S3**). Therefore, a simple, repeatable, and widely accepted plasmid transfer method for EcN is necessary. Herein, *E. coli* S17-1 λpir (ATCC BAA-2428) was selected as the donor cell because its conjugative pili system (RP4-2) is integrated into the genome for RP4-oriT-based DNA conjugation transfer.[35,36] EcN was used as a recipient (harboring control plasmid to provide another antibiotic resistance gene for transconjugant selection). After performing the conjugation workflow (**Figure 3A**), two donor plasmids (compatible with EcN control plasmids) were successfully transferred into recipient EcN strains, with conjugation efficiency of up to 10^5 CFU per 1 mL OD_{600} = 1 recipient cell (within 30 min) (**Figures 3B, C**). However, conjugation efficiency did not significantly increase after 30 min, indicating that EcN-based conjugation is a powerful and time-saving DNA transfer strategy.

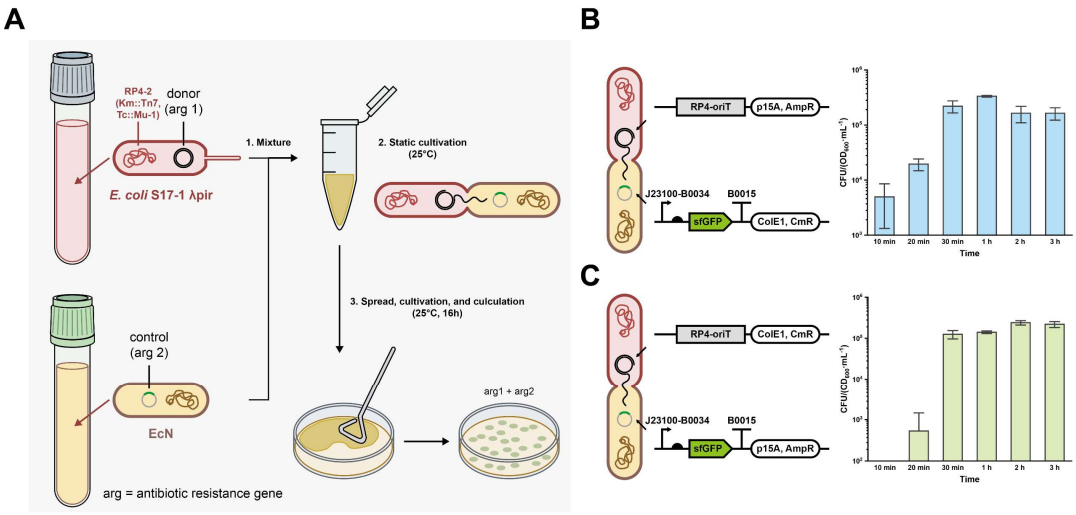

Figure 3. Bacterial conjugation.

(A) Workflow of "*E. coli* S17-1 λpir - EcN" conjugation.

(B) Conjugation efficiency of plasmid pFB345 (pFB1-RP4-oriT) transferred into EcN (harboring pFB346 as control plasmid).

(C) Conjugation efficiency of plasmid pFB347 (pSB1C3-RP4-oriT) transferred into EcN (harboring pFB348 as control plasmid).

Protein Expression Capability of EcN

Probiotic EcN has been widely used for protein expression for therapeutic applications, such as bacterial infections,[21] inflammatory bowel disease,[18] metabolic diseases,[16] and antitumor immunotherapy.[22] A higher protein expression capability is necessary because proteins act as therapeutic drugs or catalytic enzymes for metabolite production. Hence, we next attempt to explore the protein expression capability of EcN, here we select the superfolder green fluorescent protein (sfGFP) as the reporter. First, the protein expression capability of four *E. coli* strains with five constitutive σ70 promoters was compared (**Figure 4A**),[37] however, EcN had the lowest sfGFP expression level, with the highest yield of ~ 17 μg per 1 mL OD_{600} = 1 culture (**Figure 4A, right**). Then, an arabinose-inducible sfGFP expression plasmid (with different arabinose concentrations) was then established, obtaining the highest sfGFP yield of

213 ~ 8 μg per 1 mL OD_{600} = 1 culture (**Figure 4B**). Furthermore, the strong T7 RNA polymerase-
214 based protein expression systems with two compatible plasmids (one supplying low constitutive
215 T7 RNA polymerase and the other one was constructed using T7 promoter and lacI-lacO
216 transcriptional repressor system responding to isopropyl β-D-1-thiogalactopyranoside (IPTG)
217 induction) were used to improve the expression capability (**Figure 4C**).[24,38] These two kinds of
218 plasmids were coexistent in EcN, when IPTG was not added in LB medium, the leaked T7 RNA
219 polymerase caused a considerable sfGFP yield (J23113-B0034, ~ 41 μg per 1 mL OD_{600} = 1).[38]
220 When 0.5 mM was added, the highest induced sfGFP expression reached ~ 44 μg per 1 mL
221 OD_{600} = 1. In summary, three sfGFP expression systems showed that the range of EcN protein
222 expression capability is from 0.24 to 44.7 μg per 1 mL OD_{600} = 1 (**Figure 4D**), providing
223 references for EcN-based protein expression with biomanufacturing applications.
224

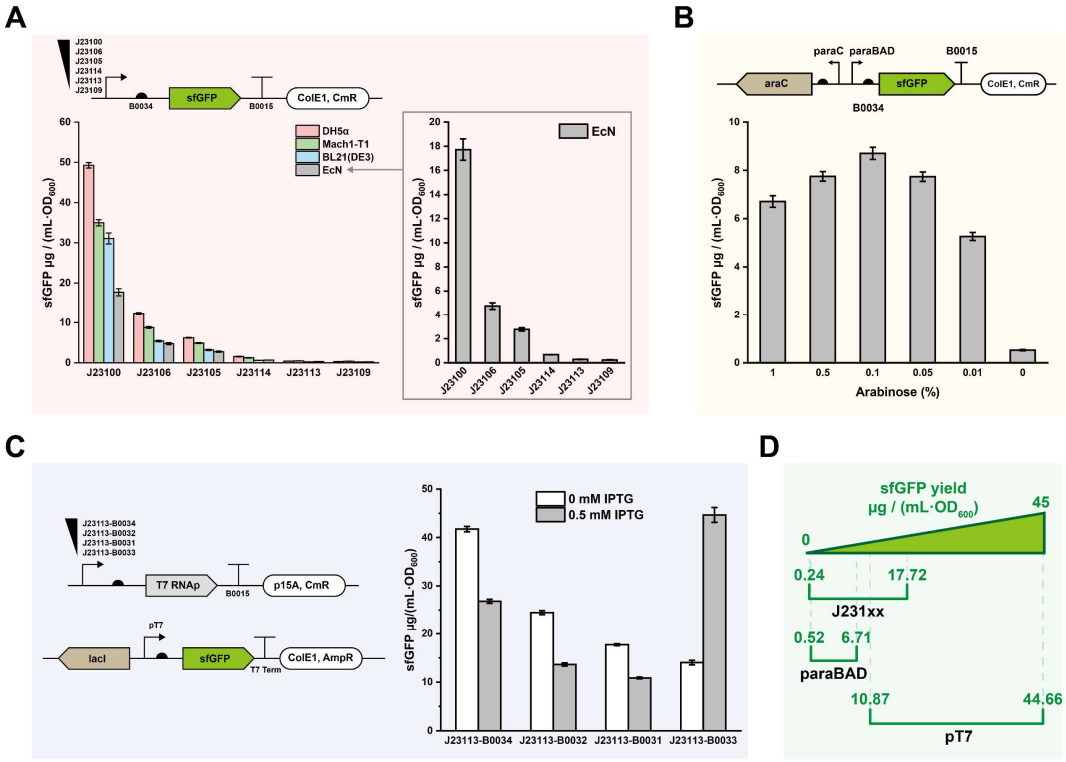

225
226

Figure 4. Quantification of EcN protein expression capability.
(A) Four *E. coli* strains (K-12 strain DH5α, W strain Mach1-T1, B strain BL21(DE3), and EcN) and six sfGFP expression plasmids (pFB346, pFB349-pFB353) were used.
(B) Arabinose-induced sfGFP expression plasmid pFB354 was used in EcN.
(C) T7 RNA polymerase expression plasmids (pFB355-pFB358) and IPTG-induced sfGFP expression plasmid (pFB359) were coexisted in EcN.
(D) sfGFP yield of all three EcN sfGFP expression systems. Each value (mean ± standard deviation, SD) was calculated with three biological replicates.

Characterization and Functionalization of EcN Native Integrases

Up to now, we performed the chassis modification and enabling technology expansion of EcN, therefore, it could be further explored as powerful platform for both *in vivo* and *in vivo* applications. Depending on our previous studies, the discovery of native integrases from EcN caught our eyes because they might be widely expanded the genetic engineering applications for defined useful purposes.[39]

Integrases are a class of enzymes that catalyze DNA-DNA site specific recombination between bacteriophage and host microbes. Bacteriophage DNA can be integrated into the host cell genome as prophage.[40] Recently, integrases have been widely developed as genetic tools in synthetic biology fields.[41] However, most of the reported integrases were isolated from non-probiotic microbes that their biosafety and acceptability were limited. Fortunately, our preliminary investigation suggested nine potential integrases in EcN genome (**Figure S4**). After analysis of comparative genome annotation (**Figure S5**), we discovered four potential prophage sequences (each prophage contains one integrase) (**Figures 5A**, **B**). Next, four arabinose-induced integrase expression plasmids were constructed to test the *in vivo* expression ability (**Figure 5C**). Notably, InterPro analysis suggested the four integrases' classification as tyrosine integrase family (**Figure S5**).[42] As a result, 6×HisTag was added in the N-terminal (DNA-

253 binding domain) rather than C-terminal (catalytic domain) to ensure the catalytic activity. Like
254 the other previously reported integrases, these four EcN native integrases could be expressed
255 as acceptable solubility (**Figure 5D**, and **Figure S6**) and purified from *E. coli* cells (**Figure 5E**).
256 Afterwards, the *attP* and *attB* sites were then reassembled (**Figure 5F**, and **Figure S7**), and
257 plasmid was constructed to characterize the integrase activity (**Figure 5G**). As expected, four
258 integrases were able to catalyze recombination events (**Figure 5H**). Furthermore, to ensure the
259 C-terminal catalytic residues, C-terminal tyrosine residues were converted into alanine or
260 phenylalanine.[43] As the InterPro annotated, the key tyrosine residues (int 1 395Y, int 2 384Y,
261 int 3 379Y, and int 4 374Y) are essential for recombination (**Figure S8**). To sum up, we
262 identified four EcN native integrases, successfully characterized their recombination activity,
263 and acquired reassembled attachment sites.
264

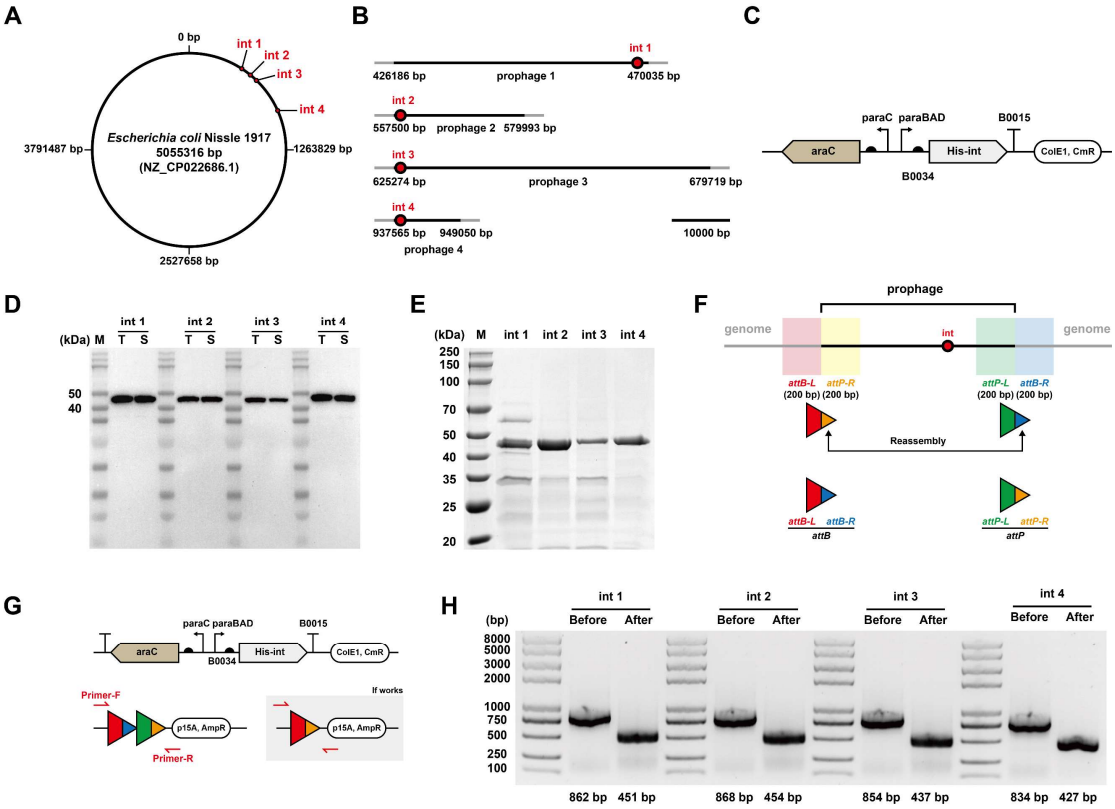

265

Figure 5. Characterization of EcN native integrases.

(A) Four potential integrases and their localization in EcN genome.

(B) Detailed prophage and integrase locations in EcN genome.

(C) Schematic of four arabinose-induced integrase expression plasmids (pFB360-pFB363).

(D) Western blot analysis of four integrases with N-terminal 6×HisTag (int 1: 50.2 kDa, int 2: 46.7 kDa, int 3: 49.6 kDa, int 4: 47.6 kDa). M: marker, T: total, S: soluble.

(E) SDS-PAGE analysis of four purified integrases.

(F) Workflow of integrase *attB* / *attP* reassembly strategy.

(G) Schematic design of integrase activity test. int 1 as an example: *E. coli* Mach1-T1 harboring both int 1 expression plasmid pFB360 and *attP* / *attB* sites plasmid pFB368 was cultured, PCR product size indicated whether int 1 performed activity.

(H) Characterization results of all four integrases. Before: PCR product without integrase catalysis, After: PCR product with integrase catalysis. All the experiments were performed as thrice with the same results.

DNA fragments can be deleted, inverted, and integrated by integrases depending on the orientation of *attP* / *attB*. Herein, the four integrases were functionalized with different *attP* / *attB* orientations. First, the reporter plasmids were designed as constitutive sfGFP expression within the same direction as *attP* / *attB* pairs to assess deletion efficiency, *E. coli* will lose fluorescence if the sfGFP is deleted by integrase (**Figure 6A**). Results showed that the four integrases had 100% deletion efficiency. Second, the reporter plasmids were designed as constitutive sfGFP expression within the opposite direction of *attP* / *attB* pairs to evaluate the inversion efficiency. A desired PCR product can be obtained if DNA is inverted, and *E. coli* may also not lose fluorescence (**Figure 6B**). Agarose gel electrophoresis results showed that the four integrases had 100% inversion efficiency (**Figure S9**). Third, to perform the integrase-mediated DNA integration, at the beginning, all four *attB* sites were initially integrated into *E. coli* MG1655 genome, then the donor plasmids were constructed with *attP* site, antibiotic resistance gene (SmR), and R6K-oriV (cannot replicate without gene *pir*)[44] (**Figure S10**). The experiments were performed with a standard protocol (**Figure 6C**), and the integration

efficiency was measured from 10^3 to 10^1 (**Figure 6D, right**). As expected, all four EcN-derived integrases were successfully functionalized as three performances: deletion, inversion, and integration.

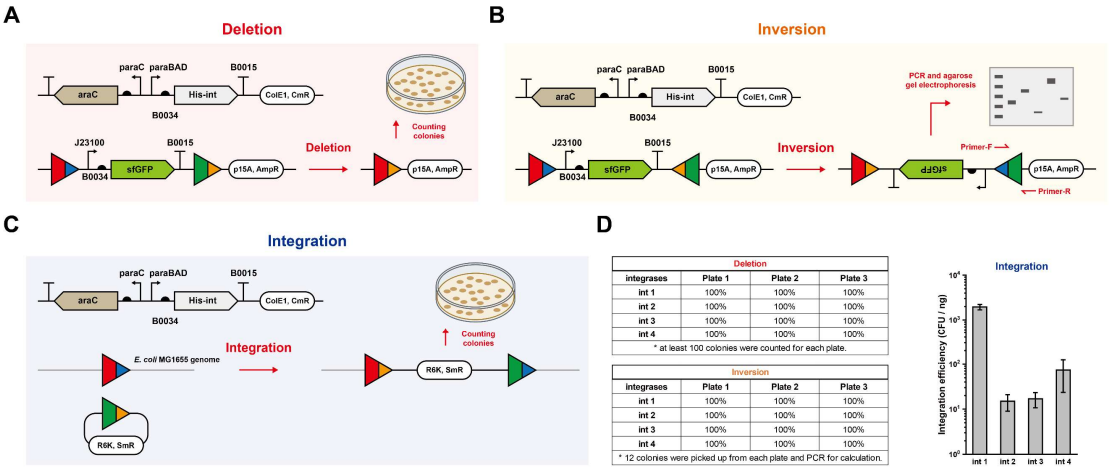

Figure 6. Functionalization of EcN native integrases.

Depending on the orientation of *attP* / *attB* sites, integrases worked as (A) deletion, (B) inversion, or (C) integration.

(D) Efficiencies of deletion, inversion, and integration. Each value (mean ± standard deviation, SD) of integration was calculated with three biological replicates.

Establishment of the Probiotic EcN-Based CFPS System

CFPS systems have been widely developed for *in vitro* protein synthesis with the advantages of time-saving, easily manipulable, microscale, high-throughput, and portable.[45] CFPS has also inspired the multidiscipline research fields, including genetic engineering,[46] metabolic engineering,[47–50] high-throughput screening,[51] pharmaceutical production,[52,53] and education.[54,55] Therefore, a powerful chassis is essential for CFPS system establishment. Several new microbial chasses, including *Pichia pastoris*,[56] *Bacillus subtilis*,[57] *Streptomyces*,[46,58–60] *Pseudomonas putida*,[61] *Vibrio natriegens*,[62,63] and *Klebsiella*

316 *pneumoniae*,[64] have been recently developed as CFPS systems. However, probiotic-based CFPS
317 systems, which have great biosafety and higher acceptability, have not been widely developed.
318 Thus, we aimed to develop a probiotic EcN-based CFPS system to expand chassis selection
319 (**Figure 7A**). Initially, we supposed to simplify the EcN genetic engineering strategy to avoid
320 complicated genetic manipulation. To meet the high-level transcription demands, we
321 constructed a series of plasmids for T7 RNA polymerase constitutive expression rather than
322 integrating T7 RNA polymerase into EcN genome (**Figure 7B**). SDS-PAGE suggested the
323 soluble expression of T7 RNA polymerase *in vivo* (**Figure 7C**). Next, EcN crude extract for
324 CFPS reactions was prepared based on the *E. coli* crude extract preparation procedure with
325 optimized parameters.[65,66] The highest sfGFP yield was 160.8 ± 6.6 μg / mL with J23114
326 promoter at 30 °C (**Figures 7D**, **E**). Furthermore, the lyophilized CFPS mixture was stored at
327 room temperature for days (**Figure 7F**), and rehydrated EcN CFPS system could produce
328 considerable sfGFP within one week (**Figure 7G**), which providing a portable probiotic-based
329 biomanufacturing platform for various applications.
330

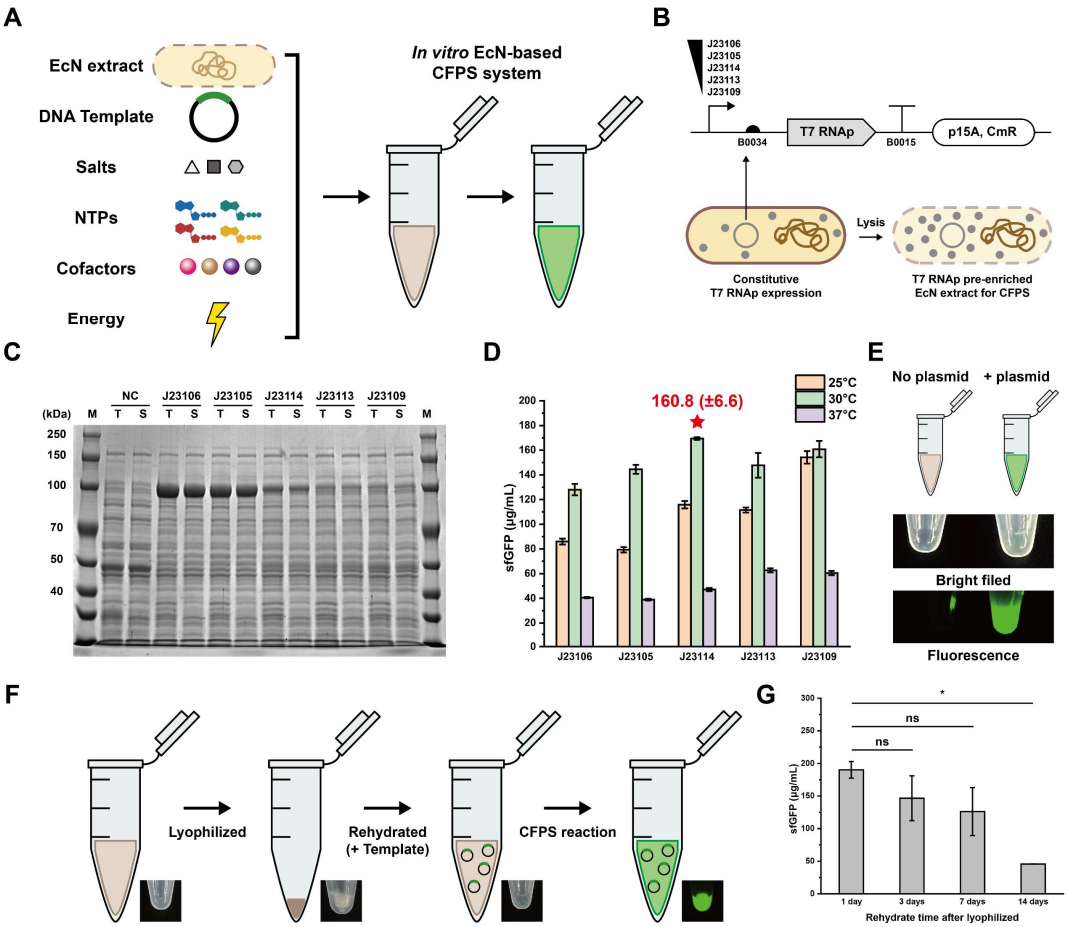

Figure 7. EcN-based cell-free protein synthesis (CFPS) system.

(A) Schematic diagram of EcN-based CFPS system.

(B) EcN strains (harboring T7 RNA polymerase constitutive expression plasmids pFB384-pFB388) for preparing CFPS crude extracts.

(C) SDS-PAGE analysis of EcN strains in (B), T7 RNA polymerase (98.9 kDa) were clearly observed. M: marker, T: total, S: soluble.

(D) sfGFP expression yield of five EcN strains and under three different temperatures for 3 h.

(E) Visualization of one 15 μL standard CFPS reaction (J23114-T7 RNA polymerase, 30 °C) under bright field and fluorescence imager.

(F) Workflow of EcN CFPS system lyophilization and rehydration.

(G) sfGFP expression yield of lyophilized EcN CFPS reactions after 1 day, 3 days, 7 days, and 14 days. Each value (mean ± standard deviation, SD) of integration was calculated with three biological replicates. Student's *t*-tests were used for statistical analysis, and $P < 0.05$ indicates statistical significance (* $P < 0.05$, "ns" means not significant).

Conclusions

As synthetic biology quickly emerged in the last twenty years, probiotics have been gradually focused as one kind of desired chassis for useful purposes.[10] Meanwhile, expanding the genetic toolbox is necessary for engineering more non-model probiotics that rarely explored.[6] In this study, EcN-based toolbox was successfully expanded from three aspects. First, we focused on the chassis modification in two ways: two EcN-based cryptic plasmids were minimized and modified as BioBrick vectors, and plasmid coexistence in EcN was extended to four compatible groups. Second, enabling technologies were developed as two methods: simplified EcN-based conjugation strategy, and capability exploration of protein expression. Third, to enrich the EcN-based applications, four EcN native integrases were successfully identified, characterized, and functionalized into genetic circuit design and genome modification *in vivo*. Furthermore, EcN-based CFPS system was established as a probiotic-based *in vitro* biomanufacturing platform.

Overall, EcN toolbox was expanded through genetic modification, DNA transfer, protein expression capability quantification, new enzyme characterization, and CFPS system establishment, which may provide convincible strategies for future probiotic engineering and related studies. Notably, two cryptic plasmids were first minimized, followed by the identification of the ColE2-oriV sequence (26 bp in pMUT2). Four probiotic-derived integrases and their activity were also assessed, enriching the integrase toolbox for genetic circuit design and gene modification purposes. Besides, this probiotic-based CFPS system may expand the *in vitro* protein expression platform with higher biosecurity, non-toxicity, and well-acceptability.

Looking forward, we expect this study can inspire the engineering of more non-model or

probiotic microbes to expand toolbox for broad applications in synthetic biology, genetic engineering, metabolic engineering, and biomedical engineering.

Methods

Strains, Vectors, Plasmids, crRNAs, Primers, and Reagents

The details of *E. coli* strains, vectors, plasmids, crRNAs, and primers used in this study are listed in **Tables S1** and **S3-S6**, **Supporting Information**. Some vectors and plasmids were derived from the author's previous works.[39,67] The complete sequences of all plasmids are listed in **Supporting Information** (**Excel Sheet Data**), and their correctness was verified by Sanger sequencing (GENEWIZ) unless otherwise noted. Q5 High-Fidelity DNA polymerase (New England Biolabs), Phanta Super-Fidelity DNA polymerase (Vazyme), FastPure Gel DNA Extraction Mini Kit (Vazyme), and pEASY - Basic Seamless Cloning and Assembly Kit (TransGen Biotech) were used for molecular cloning. DreamTaq Green PCR Master Mix (Thermo Fisher Scientific) was used for colony PCR. FastDigest Restriction Enzymes (Thermo Fisher Scientific) were used for plasmid linearization. Lysogeny broth (LB) liquid medium contained 10 g tryptone, 5 g yeast extract, and 10 g sodium chloride in 1 L ddH_2O. LB-agar plates were prepared by adding 15 g agar per liter LB liquid medium. Antibiotic stocks (1000×, dissolved in ddH_2O unless otherwise noted) were 100 mg / mL ampicillin, 50 mg / mL kanamycin, 34 mg / mL chloramphenicol (dissolved in ethanol), and 50 mg / mL streptomycin.

Genetic Parts

All genetic parts used in this study are listed in **Table S2**, **Supporting Information**.

393 Genetic parts shorter than 150 bp were synthesized within the oligonucleotides (GENEWIZ)
394 and inserted as DNA fragments during molecular cloning. Some genetic parts were derived
395 from the author's previous works.[39,67] EcN-based DNA sequences (including cryptic plasmids
396 pMUT1 / pMUT2, four integrases, and integrases-associated *attP* / *attB* sites) were gained via
397 PCR amplification referring to EcN genome sequence (GenBank: NZ_CP022686.1). RP4-oriT
398 sequence was referred to GenBank: X14165.1. All genetic parts were checked for correctness
399 with Sanger sequencing.
400
401 **Plasmid Construction**
402 All plasmids were constructed by Gibson Assembly strategy. In brief, all linear DNA
403 fragments were purified by gel extraction and then assembled by using pEASY - Basic
404 Seamless Cloning and Assembly Kit. After assembly, the reaction mixture was added to 50 μL
405 competent cells for transformation, which were incubated overnight on LB-agar plate (with
406 antibiotics for selection). After colony PCR, probable products were sequenced by Sanger
407 sequencing.
408
409 **Cryptic Plasmid Minimization**
410 DNA sequences of pMUT1 (GenBank: CP058218) and pMUT2 (GeneBank: CP058219)
411 were gained via PCR amplification (EcN whole-cell as PCR template). Minimization was
412 performed referring to both gene annotations and previous reports.[25] pMUT1-mini was
413 constructed from three DNA fragments: pMUT1-tru (partial sequence of pMUT1), CmR gene
414 (from pSB1C3), and BioBrick prefix / BioBrick suffix (oligonucleotides). pMUT2-mini was

415 constructed from three DNA fragments: pMUT2-tru (partial sequence of pMUT2), KanR gene
416 (from pKD4),[68] and BioBrick prefix / BioBrick suffix (oligonucleotides). pMUT2-based 26 bp
417 ColE2-oriV sequence was characterized by *in vivo* incremental truncation process. In brief,
418 series of truncated (200 bp, 20 bp, 4 bp, 1 bp, in steps) plasmid variants were constructed and
419 transformed into *E. coli* Mach1-T1 competent cells to determine the 5' site and 3' site of oriV.
420 (non-survival plasmid variants lack complete oriV site for plasmid replication).
421
422 **Compatible Plasmid Coexistence, Plasmid Copy Number Calculation, and Curing in EcN**
423 Each plasmid was transformed into EcN via electroporation, respectively. The EcN strains
424 with four compatible plasmids were inoculated on LB-agar plates (with four antibiotics) and
425 cultured overnight (37 °C, 16 h) to check the colony formation.
426 The copy number of each plasmid in EcN was calculated via qPCR,[39] 16s rRNA genome
427 sequence (six copies in one cell) was used as reference. The copy number per EcN cell was
428 calculated as "6 × antibiotic resistance gene copy number / 16s rRNA copy number".
429 Plasmid curing was performed as previously reported strategies,[32] in brief, the pSC101
430 oriV-derived plasmid pFB2 (high temperature sensitive) was cured by over 30 °C continuous
431 cultivation, ColE1 oriV-derived plasmids were cured by pCas, p15A and incW-oriV derived
432 plasmids were cured by "pCas + crRNA plasmids (pFB390 - pFB395)".
433
434 **Bacterial Conjugation**
435 Donor strains *(E. coli* S17-1 λpir, harboring plasmid with RP4-oriT sequence) and recipient
436 strains (EcN, harboring plasmid for antibiotic selection) were cultivated in 5 mL liquid LB

437 medium (with antibiotics) at 37 °C and 250 rpm for 16 h. On the second day, for each culture,
438 1 mL mixture (adjusted OD_{600} to ~1) was transferred into a 1.5 mL tube and centrifuged at
439 10000 g for 1 min. Then the pellets were resuspended by 1 mL LB medium (room temperature
440 25 °C, without any antibiotics) and centrifuged at 10000 g for 1 min, repeated the above wash
441 step for another two times, and then resuspended the pellets by 1 mL LB medium (room
442 temperature 25 °C, without any antibiotics). Afterwards, transferred both 50 μL donor strain
443 culture and 50 μL recipient strain culture into a new 1.5 mL tube as total 100 μL, then steadily
444 placed the mixture at 25 °C for hours. When conjugation finished, vortexed the mixture and
445 added 900 μL LB medium (room temperature 25 °C, without antibiotics) for dilution. Finally,
446 took 100 μL diluted mixture onto LB-agar plates (with two antibiotics) and cultured at 37 °C
447 for 16 h. On the third day, counting the colonies (CFU) for conjugation efficiency calculation.
448
449 ***In vivo* Fluorescence Quantification**
450 *E. coli* strains were cultivated in 5 mL liquid LB medium (with antibiotics, and with
451 arabinose or IPTG if necessary) at 37 °C and 250 rpm for 16 h. On the second day, for each
452 culture, 1 mL mixture (adjusted OD_{600} to ~1) was transferred into a 1.5 mL tube and centrifuged
453 at 10000 g for 1 min. Then the pellets were resuspended by 1 mL 1× PBS (Phosphate-buffered
454 saline, pH 7.4), and sfGFP fluorescence was measured by microplate reader (Synergy H1,
455 BioTek) and performed with excitation and emission wavelengths at 485 and 528 nm,
456 respectively. Depending on the standard curve of "sfGFP (μg / mL) - Fluorescence (a.u.)"
457 (**Figure S11**, **Supporting Information**), the *in vivo* sfGFP yield was normalized as "μg /
458 ($mL \cdot OD_{600}$)".

459

460 **Integrase Identification and Characterization**

461 Potential EcN-based native integrases were identified via comparative genome
462 annotations.[28] After the initial round of integrase searching, nine candidates (**Figure S4**,
463 **Supporting Information**) were identified and classified by InterPro.[42] Next, the supposed
464 attachment sites (both *attL* and *attR*) were analyzed, and gained relying on the potential
465 prophage location and short DNA repeats (< 20 bp, DNA core sequences for integrases
466 recombination). After reassembly *attL* / *attR* to *attP* / *attB*, plasmids were constructed for
467 functional verification of "integrase - *attP* / *attB*" pairs.

468

469 **Expression and Purification of Integrases**

470 The procedure was the same as our previous study.[39] The difference is that pFB360-
471 pFB363 were used in *E. coli* Mach1-T1 for integrase expression, and the inducer was replaced
472 by 1% w/v arabinose than 0.5 mM IPTG.

473

474 **Tyrosine Residue Mutation of Integrases**

475 Depending on the InterPro results (**Figure S5**, **Supporting Information**), the C-terminal
476 tyrosine residues were replaced by alanine or phenylalanine.[43] The tyrosine residue mutation
477 plasmids were derived from pFB360-pFB363, mutants were characterized as same as wild type.

478

479 **Functionalization of Integrases**

480 Here we describe integrase 1 as an example, the other three integrases were performed

481 similarly.

482 Deletion: *E. coli* Mach1-T1 (harboring pFB364) was transformed with pFB360, on the
483 second day, the colonies on LB-agar plates were picked up and inoculated into 5 mL liquid LB
484 medium (with two antibiotics and 1% w/v arabinose) at 37 °C and 250 rpm for 16 h. On the
485 third day, the culture was streaked onto LB-agar plates and cultured overnight at 37 °C for 16
486 h. On the fourth day, the colony's fluorescence was observed under UVP ChemStudio
487 (analytikjena), and the integrase 1-based deletion efficiency was calculated as "nonfluorescent
488 colony number / total colony number".

489 Inversion: *E. coli* Mach1-T1 (harboring pFB368) was transformed with pFB360, on the
490 second day, the colonies on LB-agar plates were picked up and inoculated into 5 mL liquid LB
491 medium (with two antibiotics and 1% w/v arabinose) at 37 °C and 250 rpm for 16 h. On the
492 third day, the culture was streaked onto LB-agar plates and cultured overnight at 37 °C for 16
493 h. On the fourth day, the colonies were picked up and performed colony PCR (forward primer:
494 int 1-inversion-F, reverse primer: VR, **Supporting Information**), if PCR product of the colony
495 matched correct size (also this colony did not lose fluorescence), this colony was successfully
496 performed the integrase 1-based inversion.

497 Integration: *E. coli* MG1655 (integrase 1 *attB* site has been inserted into the genome)
498 harboring pFB360 was inoculated into 5 mL liquid LB medium (with 1% w/v arabinose) at
499 37 °C and 250 rpm for about 3 h, when OD_{600} reached 0.6, the cell was washed by ddH_2O thrice
500 and prepared as electroporation competent cell (concentrated 10 times, OD_{600} = ~6). Then 1 ng
501 donor plasmid pFB380 was electro-transformed into 50 μL competent cell, separated onto LB-
502 agar plates (with two antibiotics), and cultured overnight at 37 °C for 16 h. On the second day,

503 the colony number (CFU) was counted, and the integrase 1-based integration efficiency was
504 calculated as CFU / ng (donor plasmid).
505
506 **Preparation of EcN Cell Extracts**
507 Cell cultivation, harvest, and lysis were prepared according to our previous reports.[66] Some
508 parameters were specially optimized for EcN Cell Extracts, the revised workflow is shown in
509 **Supporting Methods** (**Supporting Information**). The final cell extracts were stored at −80 °C
510 until use.
511
512 **Cell-Free Protein Synthesis (CFPS) and Protein Analysis**
513 Standard CFPS reactions were performed in 1.5 mL tubes with a total volume of 15 μL.
514 Each CFPS reaction contained: 12 mM magnesium glutamate, 10 mM ammonium glutamate,
515 130 mM potassium glutamate, 1.2 mM ATP, 0.85 mM each of GTP, UTP, and CTP, 34 μg / mL
516 folinic acid, 170 μg / mL of *E. coli* tRNA mixture, 2 mM each of 20 standard amino acids, 0.33
517 mM nicotinamide adenine dinucleotide (NAD), 0.27 mM coenzyme A (CoA), 1.5 mM
518 spermidine, 1 mM putrescine, 4 mM sodium oxalate, 33 mM phosphoenolpyruvate (PEP), 13.3
519 μg / mL plasmid, and 27% (v/v) of cell tract. CFPS reactions were incubated for at least 3 h,
520 and at 30 °C (unless otherwise noted). Cell-free expressed sfGFP was measured by microplate
521 reader (Synergy H1, BioTek) and performed with excitation and emission wavelengths at 485
522 and 528 nm, respectively. Depending on the standard curve of "sfGFP (μg / mL) - Fluorescence
523 (a.u.)" (**Figure S11**, **Supporting Information**), the sfGFP yield was calculated as μg / mL.
524

Lyophilization and Rehydration of EcN CFPS Mixture

Before lyophilization, each 15 μL CFPS mixture (without plasmid) was prepared and loaded into 1.5 mL tube and performed quick-freezing by liquid nitrogen. Then, the tubes were lyophilized by LABCONCO FreeZone at -70 °C, 70 Pa for at least 12 h. Next, the lyophilized CFPS mixture was stored at room temperature (25 °C) to be used. When rehydrate CFPS mixture, 15 μL nuclease free water (with plasmid) was added to tube and incubated at 30 °C for at least 3 h.

Author Information

Corresponding Author

Jian Li - School of Physical Science and Technology, ShanghaiTech University, Shanghai 201210, China; orcid.org/0000-0003-2359-238X; Email: lijian@shanghaitech.edu.cn

Authors

Fang Ba - School of Physical Science and Technology, ShanghaiTech University, Shanghai 201210, China

Yufei Zhang - School of Physical Science and Technology, ShanghaiTech University, Shanghai 201210, China

Xiangyang Ji - School of Physical Science and Technology, ShanghaiTech University, Shanghai 201210, China

Wan-Qiu Liu - School of Physical Science and Technology, ShanghaiTech University, Shanghai 201210, China

Shengjie Ling - School of Physical Science and Technology, ShanghaiTech University,

Shanghai 201210, China

Author Contributions

J.L. and F.B. designed the experiments. F.B. performed all experiments. Y.Z. helped perform molecular cloning. X.J. helped prepare cell extracts. F.B. analyzed the data and drafted the manuscript. J.L., W.-Q.L. and S.L. revised and edited the manuscript. J.L. conceived and supervised the study. All authors read and approved the final manuscript.

Acknowledgments

This work was supported by grants from the National Natural Science Foundation of China (31971348 and 32171427).

References

1. Cho, J. S.; Kim, G. B.; Eun, H.; Moon, C. W.; Lee, S. Y. Designing microbial cell factories for the production of chemicals. *JACS Au* **2022**, *2*, 1781−1799.
2. Xu, X.; Liu, Y.; Du, G.; Ledesma-Amaro, R.; Liu, L. Microbial chassis development for natural product biosynthesis. *Trends Biotechnol.* **2020**, *38*, 779−796.
3. Gurdo, N.; Volke, D. C.; McCloskey, D.; Nikel, P. I. Automating the design-build-test-learn cycle towards next-generation bacterial cell factories. *N. Biotechnol.* **2023**, *74*, 1−15.
4. Lawson, C. E.; Harcombe, W. R.; Hatzenpichler, R.; Lindemann, S. R.; Löffler, F. E.; O'Malley, M. A.; Martín, H. G.; Pfleger, B. F.; Raskin, L.; Venturelli, O. S.; Weissbrodt, D. G.; Noguera, D. R.; McMahon, K. D. Common principles and best practices for engineering microbiomes. *Nat. Rev. Microbiol.* **2019**, *17*, 725−741.
5. Zhang, C.; Liu, H.; Li, X.; Xu, F.; Li, Z. Modularized synthetic biology enabled intelligent biosensors. *Trends Biotechnol.* **2023**, DOI: 10.1016/j.tibtech.2023.03.005.
6. McCarty, N. S.; Ledesma-Amaro, R. Synthetic biology tools to engineer microbial

communities for biotechnology. *Trends Biotechnol.* **2019**, *37*, 181−197.

7. Wehrs, M.; Tanjore, D.; Eng, T.; Lievense, J.; Pray, T. R.; Mukhopadhyay, A. Engineering robust production microbes for large-scale cultivation. *Trends Microbiol.* **2019**, *27*, 524−537.
8. Cubillos-Ruiz, A.; Guo, T.; Sokolovska, A.; Miller, P. F.; Collins, J. J.; Lu, T. K.; Lora, J. M. Engineering living therapeutics with synthetic biology. *Nat. Rev. Drug Discov.* **2021**, *20*, 941−960.
9. Kelly, V. W.; Liang, B. K.; Sirk, S. J. Living Therapeutics: The next frontier of precision medicine. *ACS Synth. Biol.* **2020**, *9*, 3184−3201.
10. Pedrolli, D. B.; Ribeiro, N. V.; Squizato, P. N.; de Jesus, V. N.; Cozetto, D. A.; Team AQA Unesp at iGEM 2017. Engineering microbial living therapeutics: The synthetic biology toolbox. *Trends Biotechnol.* **2019**, *37*, 100−115.
11. Ma, J.; Lyu, Y.; Liu, X.; Jia, X.; Cui, F.; Wu, X.; Deng, S.; Yue, C. Engineered probiotics. *Microb. Cell Fact.* **2022**, *21*, 72.
12. Chen, J.; Chen, X.; Ho, C. L. Recent development of probiotic *Bifidobacteria* for treating human diseases. *Front. Bioeng. Biotechnol.* **2021**, *9*, 770248.
13. Cerbo, A. D.; Palmieri, B.; Aponte, M.; Morales-Medina, J. C.; Iannitti, T. Mechanisms and therapeutic effectiveness of lactobacilli. *J. Clin. Pathol.* **2016**, *69*, 187−203.
14. Martinović, A.; Cocuzzi, R.; Arioli, S.; Mora, D. *Streptococcus thermophilus*: To survive, or not to survive the gastrointestinal tract, that is the question! *Nutrients* **2020**, *12*, 2175.
15. Praveschotinunt, P.; Duraj-Thatte, A. M.; Gelfat, I.; Bahl, F.; Chou, D. B.; Joshi, N. S. Engineered *E. coli* Nissle 1917 for the delivery of matrix-tethered therapeutic domains to the gut. *Nat. Commun.* **2019**, *10*, 5580.
16. Isabella, V. M.; Ha, B. N.; Castillo, M. J.; Lubkowicz, D. J.; Rowe, S. E.; Millet, Y. A.; Anderson, C. L.; Li, N.; Fisher, A. B.; West, K. A.; Reeder, P. J.; Momin, M. M.; Bergeron, C. G.; Guilmain, S. E.; Miller, P. F.; Kurtz, C. B.; Falb, D. Development of a synthetic live bacterial therapeutic for the human metabolic disease phenylketonuria. *Nat. Biotechnol.* **2018**, *36*, 857−864.
17. Danino, T.; Prindle, A.; Kwong, G. A.; Skalak, M.; Li, H.; Allen, K.; Hasty, J.; Bhatia, S. N. Programmable probiotics for detection of cancer in urine. *Sci. Transl. Med.* **2015**, *7*,

603 289ra84.

604 18. Zou, Z. P.; Du, Y.; Fang, T. T.; Zhou, Y.; Ye, B. C. Biomarker-responsive engineered
605 probiotic diagnoses, records, and ameliorates inflammatory bowel disease in mice. *Cell*
606 *Host Microbe* **2023**, *31*, 1−14.

607 19. Sonnenborn, U. *Escherichia coli* strain Nissle 1917−from bench to bedside and back:
608 history of a special *Escherichia coli* strain with probiotic properties. *FEMS Microbiol. Lett.*
609 **2016**, *363*, fnw212.

610 20. Lynch, J. P.; Goers, L.; Lesser, C. F. Emerging strategies for engineering *Escherichia coli*
611 Nissle 1917-based therapeutics. *Trends Pharmacol. Sci.* **2022**, *43*, 772−786.

612 21. Deriu, E.; Liu, J. Z.; Pezeshki, M.; Edwards, R. A.; Ochoa, R. J.; Contreras, H.; Libby, S.
613 J.; Fang, F. C.; Raffatellu, M. Probiotic bacteria reduce *Salmonella* Typhimurium intestinal
614 colonization by competing for iron. *Cell Host Microbe* **2013**, *14*, 26−37.

615 22. Yu, X.; Lin, C.; Yu, J.; Qi, Q.; Wang, Q. Bioengineered *Escherichia coli* Nissle 1917 for
616 tumour-targeting therapy. *Microb. Biotechnol.* **2020**, *13*, 629−636.

617 23. Seco, E. M.; Fernández, L. Á. Efficient markerless integration of genes in the chromosome
618 of probiotic *E. coli* Nissle 1917 by bacterial conjugation. *Microb. Biotechnol.* **2022**, *15*,
619 1374−1391.

620 24. Effendi, S. S. W.; Ng, I. S. Reprogramming T7RNA polymerase in *Escherichia coli* Nissle
621 1917 under specific *Lac* operon for efficient *p*-coumaric acid production. *ACS Synth. Biol.*
622 **2022**, *11*, 3471−3481.

623 25. Kan, A.; Gelfat, I.; Emani, S.; Praveschotinunt, P.; Joshi, N. S. Plasmid vectors for *in vivo*
624 selection-free use with the probiotic *E. coli* Nissle 1917. *ACS Synth. Biol.* **2021**, *10*, 94−106.

625 26. Lan, Y. J.; Tan, S. I.; Cheng, S. Y.; Ting, W. W.; Xue, C.; Lin, T. H.; Cai, M. Z.; Chen, P. T.;
626 Ng, I. S. Development of *Escherichia coli* Nissle 1917 derivative by CRISPR/Cas9 and
627 application for gamma-aminobutyric acid (GABA) production in antibiotic-free system.
628 *Biochem. Eng. J.* **2021**, *168*, 107952.

629 27. Zainuddin, H. S.; Bai, Y.; Mansell, T. J. CRISPR-based curing and analysis of metabolic
630 burden of cryptic plasmids in *Escherichia coli* Nissle 1917. *Eng. Life Sci.* **2019**, *19*,
631 478−485.

632 28. Zhao, L.; Yin, G.; Zhang, Y.; Duan, C.; Wang, Y.; Kang, Z. A comparative study on the

633 genomes, transcriptomes, and metabolic properties of *Escherichia coli* strains Nissle 1917,
634 BL21(DE3), and MG1655. *Engineering Microbiology* **2022**, *2*, 100012.
635 29. Avison, M. B.; Walsh, T. R.; Bennett, P. M. pUB6060: A broad-host-range, DNA
636 polymerase-I-independent ColE2-like plasmid. *Plasmid* **2001**, *45*, 88−100.
637 30. Cai, Y.; Wilson, M. L.; Peccoud, J. GenoCAD for iGEM: a grammatical approach to the
638 design of standard-compliant constructs. *Nucleic Acids Res.* **2010**, *38*, 2637−2644.
639 31. Novick, R. P. Plasmid incompatibility. *Microbiol. Rev.* **1987**, *51*, 381−395.
640 32. Jiang, Y.; Chen, B.; Duan, C.; Sun, B.; Yang, J.; Yang, S. Multigene editing in the
641 *Escherichia coli* genome via the CRISPR-Cas9 system. *Appl. Environ. Microbiol.* **2015**, *81*,
642 2506−2514.
643 33. Brito, I. L. Examining horizontal gene transfer in microbial communities. *Nat. Rev.*
644 *Microbiol.* **2021**, *19*, 442−453.
645 34. Moura de Sousa, J.; Lourenco, M.; Gordo, I. Horizontal gene transfer among host-
646 associated microbes. *Cell Host Microbe* **2023**, *31*, 513−527.
647 35. Haase, J.; Lurz, R.; Grahn, A. M.; Bamford, D. H.; Lanka, E. Bacterial conjugation
648 mediated by plasmid RP4: RSF1010 mobilization, donor-specific phage propagation, and
649 pilus production require the same Tra2 core components of a proposed DNA transport
650 complex. *J. Bacteriol.* **1995**, *177*, 4779−4791.
651 36. Pansegrau, W.; Balzer, D.; Kruft, V.; Lurz, R.; Lanka, E. *In vitro* assembly of relaxosomes
652 at the transfer origin of plasmid RP4. *Proc. Natl. Acad. Sci. U. S. A.* **1990**, *87*, 6555−6559.
653 37. Beal, J.; Haddock-Angelli, T.; Baldwin, G.; Gershater, M.; Dwijayanti, A.; Storch, M.; de
654 Mora, K.; Lizarazo, M.; Rettberg, R.; with the iGEM Interlab Study Contributors.
655 Quantification of bacterial fluorescence using independent calibrants. *PLoS One* **2018**, *13*,
656 e0199432.
657 38. Tan, S. I.; Ng, I. S. New insight into plasmid-driven T7 RNA polymerase in *Escherichia*
658 *coli* and use as a genetic amplifier for a biosensor. *ACS Synth. Biol.* **2020**, *9*, 613−622.
659 39. Ba, F.; Liu, Y.; Liu, W. Q.; Tian, X.; Li, J. SYMBIOSIS: synthetic manipulable biobricks
660 via orthogonal serine integrase systems. *Nucleic Acids Res.* **2022**, *50*, 2973−2985.
661 40. Grindley, N. D.; Whiteson, K. L.; Rice, P. A. Mechanisms of site-specific recombination.
662 *Annu. Rev. Biochem.* **2006**, *75*, 567−605.

663 41. Merrick, C. A.; Zhao, J.; Rosser, S. J. Serine integrases: Advancing synthetic biology. *ACS*
664 *Synth. Biol.* **2018**, *7*, 299−310.
665 42. Paysan-Lafosse, T.; Blum, M.; Chuguransky, S.; Grego, T.; Pinto, B. L.; Salazar, G.A.;
666 Bileschi, M. L.; Bork, P.; Bridge, A.; Colwell, L.; Gough, J.; Haft, D. H.; Letunić, I.;
667 Marchler-Bauer, A.; Mi, H.; Natale, D. A.; Orengo, C. A.; Pandurangan, A. P.; Rivoire, C.;
668 Sigrist, C. J.; Sillitoe, I.; Thanki, N.; Thomas, P. D.; Tosatto, S. C.; Wu, C. H.; Bateman, A.
669 InterPro in 2022. *Nucleic Acids Res.* **2023**, *51*, D418−D427.
670 43. Evans, B. R.; Chen, J. W.; Parsons, R. L.; Bauer, T. K.; Teplow, D. B.; Jayaram, M.
671 Identification of the active site tyrosine of Flp recombinase. Possible relevance of its
672 location to the mechanism of recombination. *J. Biol. Chem.* **1990**, *265*, 18504−18510.
673 44. Rakowski, S. A.; Filutowicz, M. Plasmid R6K replication control. *Plasmid* **2013**, *69*,
674 231−242.
675 45. Liu, W. Q.; Zhang, L.; Chen, M.; Li, J. Cell-free protein synthesis: Recent advances in
676 bacterial extract sources and expanded applications. *Biochem. Eng. J.* **2019**, *141*, 182−189.
677 46. Xu, H.; Yang, C.; Tian, X.; Chen, Y.; Liu, W. Q.; Li, J. Regulatory part engineering for high-
678 yield protein synthesis in an all-*Streptomyces*-based cell-free expression system. *ACS Synth.*
679 *Biol.* **2022**, *11*, 570−578.
680 47. Zhuang, L.; Huang, S.; Liu, W. Q.; Karim, A. S.; Jewett, M. C.; Li, J. Total *in vitro*
681 biosynthesis of the nonribosomal macrolactone peptide valinomycin. *Metab. Eng.* **2022**, *60*,
682 37−44.
683 48. Rasor, B. J.; Karim, A. S.; Alper, H. S.; Jewett, M. C. Cell extracts from bacteria and yeast
684 retain metabolic activity after extended storage and repeated thawing. *ACS Synth. Biol.*
685 **2023**, *12*, 904−908.
686 49. Liu, Y.; Liu, W. Q.; Huang, S.; Xu, H.; Lu, H.; Wu, C.; Li, J. Cell-free metabolic engineering
687 enables selective biotransformation of fatty acids to value-added chemicals. *Metab. Eng.*
688 *Commun.* **2023**, *16*, e00217.
689 50. Chen, Y.; Liu, W. Q.; Zheng, X.; Liu, Y.; Ling, S.; Li, J. Cell-free biosynthesis of lysine-
690 derived unnatural amino acids with chloro, alkene, and alkyne groups. *ACS Synth. Biol.*
691 **2023**, *12*, 1349−1357.
692 51. Karim A. S.; Dudley, Q. M.; Juminaga, A.; Yuan, Y.; Crowe, S. A.; Heggestad, J. T.; Garg,

693 S.; Abdalla, T.; Grubbe, W. S.; Rasor, B. J.; Coar, D. N.; Torculas, M.; Krein, M.; Liew, F.
694 E.; Quattlebaum, A.; Jensen, R. O.; Stuart, J. A.; Simpson, S. D.; Köpke, M.; Jewett, M. C.
695 *In vitro* prototyping and rapid optimization of biosynthetic enzymes for cell design. *Nat.*
696 *Chem. Biol.* **2020**, *16*, 912−919.
697 52. Ji, X.; Liu, W. Q.; Li, J. Recent advances in applying cell-free systems for high-value and
698 complex natural product biosynthesis. *Curr. Opin. Microbiol.* **2022**, *67*, 102142.
699 53. Meng, Y.; Yang, M.; Liu, W. Q.; Li, J. Cell-free expression of a therapeutic protein
700 serratiopeptidase. *Molecules* **2023**, *28*, 3132.
701 54. Stark, J.C.; Huang, A.; Nguyen, P. Q.; Dubner, R. S.; Hsu, K. J.; Ferrante, T. C.; Anderson,
702 M.; Kanapskyte, A.; Mucha, Q.; Packett, J. S.; Patel, P.; Patel, R.; Qaq, D.; Zondor, T.;
703 Burke, J.; Martinez, T.; Miller-Berry, A.; Puppala, A.; Reichert, K.; Schmid, M.; Brand, L.;
704 Hill, L. R.; Chellaswamy, J. F.; Faheem, N.; Fetherling, S.; Gong, E.; Gonzalzles, E. M.;
705 Granito, T.; Koritsaris, J.; Nguyen, B.; Ottman, S.; Palffy, C.; Patel, A.; Skweres, S.; Slaton,
706 A.; Woods, T.; Donghia, N.; Pardee, K.; Collins, J. J.; Jewett, M. C. BioBits Bright: A
707 fluorescent synthetic biology education kit. *Sci. Adv.* **2018**, *4*, eaat5107.
708 55. Huang, A.; Nguyen, P. Q.; Stark, J. C.; Takahashi, M. K.; Donghia, N.; Ferrante, T.; Dy, A.
709 J.; Hsu, K. J.; Dubner, R. S.; Pardee, K.; Jewett, M. C.; Collins, J. J. BioBits Explorer: A
710 modular synthetic biology education kit. *Sci. Adv.* **2018**, *4*, eaat5105.
711 56. Zhang, L.; Liu, W. Q.; Li, J. Establishing a eukaryotic *Pichia pastoris* cell-free protein
712 synthesis system. *Front. Bioeng. Biotechnol.* **2020**, *8*, 536.
713 57. Kelwick, R.; Webb, A. J.; MacDonald, J. T.; Freemont, P. S. Development of a *Bacillus*
714 *subtilis* cell-free transcription-translation system for prototyping regulatory elements.
715 *Metab. Eng.* **2016**, *38*, 370−381.
716 58. Xu, H.; Liu, W. Q.; Li, J. Translation related factors improve the productivity of a
717 *Streptomyces*-based cell-free protein synthesis system. *ACS Synth. Biol.* **2020**, *9*,
718 1221−1224.
719 59. Li, J.; Wang, H.; Kwon, Y. C.; Jewett, M. C. Establishing a high yielding *Streptomyces*-
720 based cell-free protein synthesis system. *Biotechnol. Bioeng.* **2017**, *114*, 1343−1353.
721 60. Li, J.; Wang, H.; Jewett, M. C. Expanding the palette of *Streptomyces*-based cell-free
722 protein synthesis systems with enhanced yields. *Biochem. Eng. J.* **2018**, *130*, 29−33.

61. Wang, H.; Li, J.; Jewett, M. C. Development of a *Pseudomonas putida* cell-free protein synthesis platform for rapid screening of gene regulatory elements. *Synth. Biol.* **2018**, *3*, ysy003.

62. Des Soye, B. J.; Davidson, S. R.; Weinstock, M. T.; Gibson, D. G.; Jewett, M. C. Establishing a high-yielding cell-free protein synthesis platform derived from *Vibrio natriegens*. *ACS Synth. Biol.* **2018**, *7*, 2245−2255.

63. Wiegand, D. J.; Lee, H. H.; Ostrov, N.; Church, G. M. Establishing a cell-free *Vibrio natriegens* expression system. *ACS Synth. Biol.* **2018**, *7*, 2475−2479.

64. Yang, C.; Yang, M.; Zhao, W.; Ding, Y.; Wang, Y.; Li, J. Establishing a *Klebsiella pneumoniae*-based cell-free protein synthesis system. *Molecules* **2022**, *27*, 4684.

65. Kwon, Y. C.; Jewett, M. C. High-throughput preparation methods of crude extract for robust cell-free protein synthesis. *Sci. Rep.* **2015**, *5*, 8663.

66. Liu, W. Q.; Wu, C.; Jewett, M. C.; Li, J. Cell-free protein synthesis enables one-pot cascade biotransformation in an aqueous-organic biphasic system. *Biotechnol. Bioeng.* **2020**, *117*, 4001−4008.

67. Ba, F.; Ji, X.; Huang, S.; Zhang, Y.; Liu, W. Q.; Liu, Y.; Ling, S.; Li, J. Engineering *Escherichia coli* to utilize erythritol as sole carbon source. *Adv. Sci.* **2023**, *10*, 2207008.

68. Datsenko, K. A.; Wanner, B. L. One-step inactivation of chromosomal genes in *Escherichia coli* K-12 using PCR products. *Proc. Natl. Acad. Sci. U. S. A.* **2000**, *97*, 6640−6645.

For Table of Contents Use Only

Expanding the toolbox of probiotic *Escherichia coli* Nissle 1917 for synthetic biology

Fang Ba, Yufei Zhang, Xiangyang Ji, Wan-Qiu Liu, Shengjie Ling, and Jian Li*

School of Physical Science and Technology, ShanghaiTech University, Shanghai, 201210, China

*Corresponding author. Email: lijian@shanghaitech.edu.cn (J.L.)